Pressure of Neon, Argon, and Xenon Bubbles in Aluminum

A. vom Felde, J. Fink, Th. Müller-Heinzerling, J. Pflüger, B. Scheerer, and G. Linker
Institut für Nukleare Festkörperphysik, Kernforschungszentrum Karlsruhe, D-7500 Karlsruhe, Federal Republic of Germany

and

D. Kaletta
Institut für Material- und Festkörperforschung, Kernforschungszentrum Karlsruhe, D-7500 Karlsruhe, Federal Republic of Germany

(Received 27 February 1984)

Neon, argon, and xenon bubbles in aluminum have been investigated by means of electron-energy-loss spectroscopy and transmission electron microscopy. The density and pressure in the bubbles were determined from the pressure shift of the $^1S_0$-$^1P_1$ transition of the rare gases as well as from analysis of electron-diffraction patterns. The experiments yield overpressurized bubbles, containing liquid Ne and solid Ar and Xe at room temperature. In the case of Xe, epitaxial growth of the rare gas in the Al matrix was observed.

PACS numbers: 61.80.Jh, 61.14.Fe, 62.50.+p, 71.45.Gm

Rare gases in metals produced by nuclear reaction or by ion implantation are essentially insoluble[1] and hence tend to precipitate and to form bubbles. The pressure in the bubbles yields information on their energetics and formation kinetics. Investigations carried out previously on He bubbles by different authors yielded pressure values which were not in agreement. Several techniques, such as vacuum-ultraviolet absorption spectroscopy[2,3] or energy-loss spectroscopy (ELS)[2-6] have been used to study the pressure shift of the He 1^1S_0-2^1P_1 transition. From these investigations the existence of bubbles overpressurized with respect to the thermal equilibrium value, where the pressure is balanced by the surface tension, was deduced. Similar results were obtained from small-angle x-ray scattering measurements.[7,8] On the other hand, recent calculations of the proportionality constant relating the density and the pressure shift of the He 1^1S_0-2^1P_1 transition yield pressures near the thermal equilibrium value.[9,10] Thus the existence of overpressurized bubbles is still highly controversial, although they had been predicted theoretically in 1959.[11] In order to clarify this question and because up to now only scarce information about non-He rare-gas bubbles in metals has been obtained, an ELS investigation of Ne, Ar, and Xe bubbles in aluminum was started. From the blue shift of the valence electron excitation ($^1S_0$-$^1P_1$) in Ne and Ar the pressures in the bubbles were derived. Valence electron excitation in xenon is coupled with the bubble surface plasmon, preventing an analogous derivation. In addition, contributions from the rare gases were observed in the elastic diffraction patterns taken with an ELS spectrometer as well as with an electron microscope. In the case of solid rare gas in the bubbles, these contributions can be interpreted as Bragg reflexes. Lattice constants and thus densities and pressures can be derived.

Epitaxially grown aluminum films with a grain size of about 2000 Å and with a thickness of almost 1000 Å were produced by evaporation of Al on a NaCl(100) surface. A homogeneous distribution of the rare-gas atoms in the Al host matrix was realized by implanting at room temperature with different energies and doses. The total amount of implanted Ne, Ar, and Xe was in all cases 3 at.%. In the case of Ar and Xe, the trapped amount was determined by Rutherford backscattering measurements to be 2.0 and 2.2%, respectively. Transmission ELS measurements at room temperature were performed with a high-resolution 170-keV spectrometer. The energy and momentum resolutions were 0.14 eV and 0.04 $Å^{-1}$, respectively. Transmission electron microscope (TEM) studies of the bubble radii, given in Table I, and their distributions were performed in a Philips EM 400 T microscope.

Figure 1 shows the energy-loss spectra of the *Al*Ne, *Al*Ar, and *Al*Xe samples in the energy region from 0 to 20 eV. Loss maxima at 15 and 6.8 eV can be ascribed to the Al volume and surface plasmons.[12] In the *Al*Ne spectrum a further plasmon occurring at 11.7 eV originates from the electron oscillations on the bubble surfaces.[13] The features at 18.3 eV correspond to the $^1S_0$-$^1P_1$ transition of the $2p$ electron of neon[14,15] which is blue shifted by an amount of 1.4 eV compared to its atomic value. The argon bubble surface plasmon is located at 10.2 eV as a consequence of the greater dielectric constant of argon in comparison with neon.[13] The $^1S_0$-$^1P_1$ transition occurs at 12.8 eV,

TABLE I. Radii, densities, and pressures of rare-gas bubbles in Al and pressure for liquid-solid transition of the rare gas. Subscript ΔE: from energy shift of valence excitations. Subscript Δk: from diffraction patterns. Subscript ls: liquid-solid.

	*Al*Ne	*Al*Ar	*Al*Xe
r (Å)	13	15	13
$n_{\Delta E}$ (Å^{-3})	0.073	0.04	...
$n_{\Delta k}$ (Å^{-3})	...	0.035	0.023
$P_{\Delta E}$ (kbar)	40 (27)	60 (35)	...
$P_{\Delta k}$ (kbar)	...	30	30
P_{ls} (kbar)	48	12	5

which is 1 eV above the corresponding atomic value.[16,17] Surprisingly the *Al*Xe spectrum does not exhibit a bubble surface plasmon although the Xe bubbles are found in TEM images. The reason is that in the energy region from 7–11 eV, where the plasmon is expected to appear, additional energy losses due to Xe valence excitations exist.[18–20] The coupling of both these oscillations leads to a damping of the bubble surface plasmon and to a distortion of the normal loss spectra of Xe, which can be well understood on the basis of an effective-medium theory.[21] Decoupling was achieved for samples annealed at 625 °C by measuring the energy loss at nonzero momentum transfer q. In this case, the scattering process is confined to a space region smaller than the bubble radius. To a first approximation, either scattering in the bubble or scattering in the matrix is observed. For $q \geq 0.2$ Å^{-1} three distinct Xe excitations without a measurable shift compared to atomic Xe are observable. The fact that these transitions are not shifted is in agreement with the observation that there is no shift in transition energy between solid and gaseous Xe.

Figure 2 presents the diffraction spectra of the *Al*Ne, *Al*Ar, and *Al*Xe samples taken by the energy-loss spectrometer in a momentum-transfer range q from 0.7 to 3.6 Å^{-1}. Besides the narrow Al(111) and Al(200) reflections broad maxima appear at smaller q which are also detectable in TEM diffraction images as diffuse rings. Clear evidence was found that these features arise from diffraction at the rare-gas bubbles and that for Ar and Xe the maxima can be ascribed to the (111) reflections of solid rare gas crystallized in fcc structure. Note, for example, that going from Ne to Xe, i.e., towards higher atomic volume, the maximum shifts by a corresponding amount to smaller q values, or that annealing of the sample causes bubble growth, and hence density decrease, which likewise results in a shift. In the case of Xe ELS and TEM scattering experiments also showed that the intensities of the

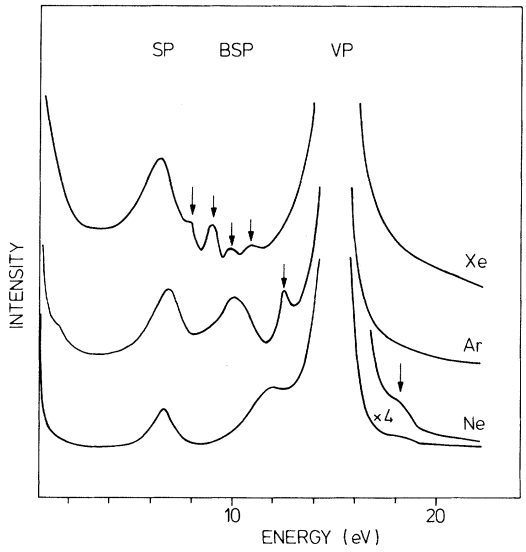

FIG. 1. Energy-loss spectra of Al films implanted with about 3 at.% Ne, Ar, and Xe, at insignificant momentum transfer q. The *Al*Ar and the *Al*Xe spectra are taken on annealed samples. SP: Al-surface plasmon. BSP: bubble surface plasmon. VP: volume plasmon of Al. Arrows indicate valence electron transitions of the rare-gas atoms.

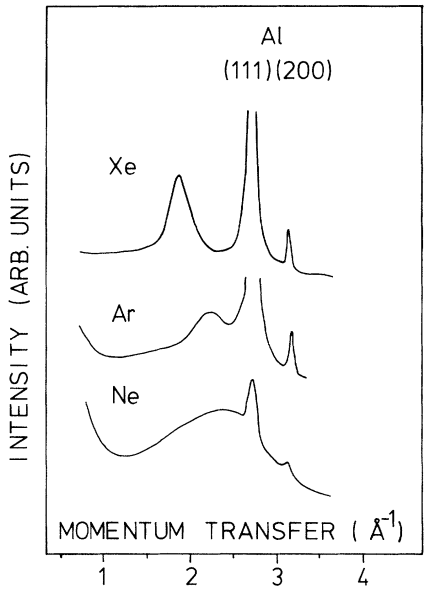

FIG. 2. Diffraction patterns of Al films implanted with about 3 at.% Ne, Ar, and Xe, taken with an ELS spectrometer. Al(111) and Al(200) are indicated. At q near 2 Å^{-1}, contributions of the rare-gas bubbles are observed.

Xe(111) reflections are correlated with the intensity of the Al(111) reflections which indicated an epitaxial growth of the solid Xe in the Al matrix. Moreover, in the case of Xe, also higher-order reflections have been identified. The considerable width of the Ar and Xe peaks can be understood as a result of scattering from small objects. A calculation of the structure factor[22] of a sphere with a radius of 15 Å yields a half-width of the (111) reflection of about 0.25 $Å^{-1}$. The difference from the experimentally observed half-widths of 0.3–0.4 $Å^{-1}$ may be caused by a distribution of pressures and hence lattice constants in the rare-gas bubbles. The considerable width of the peak in the *Al*Ne spectrum suggests that the neon is liquid. Finally, the relative intensity of the maximum is strongly reduced for Ne compared to Xe, as is expected because the elastic-scattering cross section is proportional to Z^2. This is also the reason why we could not observe such maxima in He-implanted films. The other reason why it is so difficult to see Bragg reflections from He bubbles is that small bubbles and thus low implantation doses, i.e., low He content, are necessary to produce solid He.[4]

To calculate density values from the pressure-induced energy shifts, a linear relationship between shift and density is assumed.[5,9,10] The proportionality constant is obtained from a comparison of the shift from the $^1S_0$-$^1P_1$ atomic to the corresponding solid transition energy with the corresponding densities. The calculated proportionality constants are 19 eV $Å^3$ for Ne and 25 eV $Å^3$ for Ar. An equation of state relates pressures, shown in Table I, to the calculated density values.[23,24] Moreover, in the case of *Al*Ne and *Al*Ne Hartree calculations of the pressure dependence of the $^1S_0$-$^1P_1$ transition energy exist[25,26] and yield the proportionality constants 20 and 26.4 eV $Å^3$, respectively. The corresponding pressures are given in Table I in parentheses.

In the case of Ar and Xe, where we believe the rare gas to be solid with a fcc structure, a careful analysis of the scattering spectra of *Al*Ar and *Al*Xe yields the lattice parameters of the solid rare gas in the bubble. Then again densities and, by means of equations of states,[23,24] pressures in the bubbles can be derived. The values are listed in Table I. For the interpretation of the neon spectra, a molecular-dynamics calculation of the pressure-dependent structure factor of liquid neon is in process.

The pressure values are subject to considerable errors, introduced by very small energy differences from which the proportionality constants were calculated; in addition to that, a small error in density causes a great error in the corresponding pressure. Nevertheless, density and pressure values determined in this way are of comparable size and consistent with our assumption of solid Ar and Xe and liquid Ne. The fact that the values are similar in magnitude is to be expected for bubbles with a certain radius in the same matrix, because the pressure in the bubbles should be independent of the implanted rare gas, but should depend on the host matrix and be inversely proportional to the bubble radius. The mean bubble radii only slightly differ from one sample to another.

It is interesting to remember here the results obtained for *Al*He samples[4–6] by that group which found the bubbles to be overpressurized. A pressure of 130 kbar was calculated for bubbles with a mean radius of 6.5 Å, i.e., He bubbles with a radius of 15 Å should be pressurized at about 60 kbar. This is close to the pressure values presented here, which are all in the range of 40 kbar.

If the bubbles are growing by the absorption of thermal vacancies, they will relax to the thermal equilibrium pressure, $p = 2\gamma/r$, where γ is the surface free energy and r the bubble radius. The results show in all cases the existence of overpressurized bubbles, i.e., all pressures obtained exceed the thermal equilibrium pressure, which is 13 kbar for bubbles in Al having a radius of 15 Å. The results may also be understood as support for the theory of Greenwood, Foreman, and Rimmer,[11] which states that for temperatures smaller than one-half of the melting temperature the growth of the bubbles, and thus the pressure, is controlled by the emission of dislocation loops. This pressure is given[27] by

$$p \lesssim \frac{2\gamma}{r} + \frac{\mu b}{2\pi r}\ln\frac{r}{r_D} \cong \frac{2\gamma}{r} + \frac{\mu b}{r} = 60 \text{ kbar},$$

where $\mu \cong 2.6\times 10^{10}$ Pa is the shear modulus of Al, $b = 2.3$ Å ($\vec{b} \parallel \langle 111\rangle$) is the Burgers vector of Al, and $r_D \cong 0.1$ b.

Note that controversy concerning the pressure arose to some extent from the difference in relating density values to observed line shifts. However, in this paper we have used a new way to determine density and pressure values, viz., from analyzing electron-diffraction patterns. In the case of *Al*He this method was not applicable because of the low-scattering amplitude of He in comparison to Ne or even Xe. However, because of the fact that electron diffraction is applicable to non-He rare-gas bubbles in Al the possibility is offered to gain insight into the structure of the rare gas in the matrix. As a fascinating example we mention *Al*Xe: Our

experiments reveal for the first time the existence of epitaxially grown rare-gas bubbles in the Al matrix. To understand the mechanism for this epitaxial growing, further experimental work is necessary.

We are indebted to H. Rietschel and R. von Baltz for many helpful discussions.

[1]J. von den Driesch and P. Jung, High Temp. High Pressures **12**, 635 (1980).

[2]J. C. Rife, S. E. Donelly, J.-M. Gilles, A. A. Lucas, and J. J. Ritsko, Phys. Rev. Lett. **46**, 1220 (1981).

[3]S. E. Donelly, J. G. Rife, J.-M. Gilles, and A. A. Lucas, J. Nucl. Mater. **93&94**, 767 (1980).

[4]R. Manzke, W. Jäger, H. Trinkaus, G. Crecelius, R. Zeller, and J. Fink, Solid State Commun. **44**, 481 (1982).

[5]W. Jäger, R. Manzke, H. Trinkaus, R. Zeller, J. Fink, and G. Crecelius, Radiat. Eff. **78**, 315 (1983).

[6]W. Jäger, R. Manzke, H. Trinkaus G. Crecelius, R. Zeller, J. Fink, and H. L. Bay, J. Nucl. Mater. **111&112**, 674 (1982).

[7]H. G. Haubold and J. S. Lin, J. Nucl. Mater. **111&112**, 709 (1982).

[8]H. G. Haubold, Radiat. Eff. **78**, 385 (1983).

[9]A. A. Lucas, J. P. Vigneron, Ph. Lambin, S. E. Donelly, and J. C. Rife, Radiat. Eff. **78**, 349 (1983).

[10]S. E. Donelly, A. A. Lucas, J. P. Vigneron, and J. C. Rife, Radiat. Eff. **78**, 337 (1983).

[11]G. W. Greenwood, A. J. E. Foreman, and D. E. Rimmer, J. Nucl. Mater. **4**, 305 (1959).

[12]H. Raether, in *Excitation of Plasmons and Interband Transitions by Electrons,* Springer Tracts in Modern Physics, edited by G. Höhler and E. A. Niekisch, Vol. 88 (Springer, New York, 1980), pp. 138–139.

[13]M. Natta, Solid State Commun. **7**, 823 (1969).

[14]J. Daniels and P. Krüger, Phys. Status Solidi (b) **43**, 659 (1971).

[15]L. Schmidt, Phys. Lett. **36A**, 87 (1971),

[16]H. Börsch and J. Geiger, Phys. Lett. **3**, 64 (1962).

[17]O. Bostanjoglo and L. Schmidt, Phys. Lett. **22**, 130 (1966).

[18]P. Keil, Z. Phys. **214**, 251 (1968).

[19]P. Keil, Z. Naturforsch. **21A**, 503 (1966).

[20]J. Geiger, Z. Phys. A **282**, 129 (1977).

[21]A. vom Felde, J. Fink, and J. Pflüger, to be published.

[22]A. Guinier, *X-ray Diffraction* (Freeman, San Francisco, 1963), p. 323.

[23]L. W. Finger, R. M. Hazen, G. Zou, H. K. Mao, and P. M. Bell, Appl. Phys. Lett. **39**, 892 (1981).

[24]K. Syassen and W. B. Holzapfel, Phys. Rev. B **18**, 5826 (1978).

[25]M. Derbyshire and R. D. Etters, J. Chem. Phys. **79**, 831 (1983).

[26]R. LeSar, Phys. Rev. B **28**, 6812 (1983).

[27]H. Trinkaus, Radiat. Eff. **78**, 189 (1983).